# Using Different Preparation Methods to Enhance Fischer-Tropsch Products over Iron-based Catalyst

**M. Sarkari[a,b], F. Fazlollahi[b], H. Atashi[c,*], A. A. Mirzaei[d], and W. C. Hecker[b]**

[a]South Pars Gas Complex Company, Asalooyeh, Iran

[b]Chemical Engineering Department, Brigham Young University, Provo, UT 84602, USA

[c]Department of Chemical Engineering, Faculty of Engineering, University of Sistan and Baluchestan, P.O. Box 98164–161, Zahedan, Iran

[d]Department of Chemistry, Faculty of Science, University of Sistan and Baluchestan, P.O. Box 98135–674, Zahedan, Iran

Original scientific paper
Received: September 23, 2012
Accepted: February 25, 2013

Three Fe-Mn/$Al_2O_3$ catalysts were prepared by three different preparation techniques, i.e. co-precipitation; sol-gel and impregnation, and their Fischer–Tropsch Synthesis (FTS) activity and selectivity behavior were investigated and compared using a fixed-bed reactor. It was observed that the impregnated catalyst had the lowest initial activity but was more stable than the other catalysts. The co-precipitated and sol-gel catalysts showed enhanced light olefin production as compared with the impregnated. Methane selectivity decreased with time on stream for both the impregnated and co-precipitated catalysts while it increased for the sol-gel. The impregnated catalyst showed the lowest WGS activity, the highest hydrocarbon selectivity and the highest chain growth probability.

*Key words:*
Fischer–Tropsch Synthesis, Fe-Mn/$Al_2O_3$ catalyst, co-precipitation, sol-gel, impregnation

## Introduction

Recently, the world energy crisis, high oil prices, and environmental pollution have received remarkable attention in the development of alternative technology (i.e. GTL) for the manufacture of transportation fuels.[1–3] In the GTL process, Fischer–Tropsch synthesis (FTS) plays an important role for converting synthesis gas (mixture of CO and $H_2$) in the production of ultra-clean transportation fuels, chemicals, and other hydrocarbon products. The development of an effective catalyst and reactor system is the most competitive issue in FTS. The catalysts mainly used for FTS are iron and cobalt. Iron is an active FTS catalyst and also for water-gas-shift (WGS) reaction and is therefore ideal for converting carbon monoxide-lean syngas (low $H_2$/CO ratio) derived from coal.[4–5]

Higher activity, selectivity and stability can be noticed in mixed metal catalysts compared to single component ones[6] whereas catalyst composition exerts the greatest influence on the molecular weight distribution. Also, it is accepted that due to thermodynamic and kinetic limitations of the reactions, bimetallic catalysts system is more capable to enhance the value of the light olefins.[7–10]

A number of studies have indicated improved activity and/or selectivity on the addition of transition metals to Fe-based FTS catalysts.[11–14] Lohitharn and Goodwin Jr.[15] showed that the addition of various transition metals besides Cu, such as Zr, Cr, Mo, Mn, Ta and V, greatly increased the catalyst activities for both CO hydrogenation and WGS in varying degrees.[16]Among the promoted iron-based catalysts, Fe-Mn catalyst is of industrial interest that has been described extensively in recent years due to its higher olefin and middle distillate selectivity.

The addition of moderate amounts of Mn has been found to promote the activity of Fe catalysts,[16–17] the formation of low-molecular weight olefins,[11,12,16,17] higher hydrocarbon formation,[18] and catalyst stability.[11] In addition, promotion of an iron catalyst with small amounts of Mn has been demonstrated to improve the surface basicity and carburization of Fe.[17,18] Some researchers declare that by using an optimum amount of Mn, the catalyst activity, stability and selectivity to $C_5$–$C_{10}$ increase while $CO_2$ and methane selectivity decreases; catalysts with high content of Mn have relatively stable activity. However, van Dijk et al.,[19] in their studies of

*Corresponding author, Tel.: + 98 9121193366;
E-mail address: h.ateshy@hamoon.usb.ac.ir (H. Atashi).

Fe-Mn catalysts with various manganese contents, found that no relationship exists between the olefin selectivity and the amount of manganese added. The catalytic behavior of mixed iron-manganese oxides was found to be influenced by the preparation technique and the structural properties of the catalytic precursors.[20]

In this study, three Fe-Mn/$Al_2O_3$ catalysts were prepared by three different preparation techniques i.e. co-precipitation; sol-gel and impregnation to investigate activity and selectivity behavior during the FTS in a fixed-bed reactor.

## Experimental section

### Catalyst preparation

In previous study[21] it was noticed that the co-precipitate catalyst containing 50%Fe/50%Mn/5wt.%$Al_2O_3$ is an optimum-modified catalyst for the conversion of synthesis gas to light olefins. The actual phases identified in the fresh catalyst were $Mn_3O_8$ (monoclinic), $Fe_2O_3$ (rhombohedral), and $Mn_2O_3$ (cubic) and in the tested catalyst, different phases including FeO (cubic), MnO (cubic), $Fe_3O_4$, and $Fe_2C$ (orthorhombic) were identified. In the present work, we prepared catalysts with the same composition (Fe:Mn = 1:1 mol ratio) using sol-gel and wetness impregnation technique in the following way to study its catalytic performance during the FTS.

For sol–gel catalyst, $Mn(NO_3)_2 \cdot 4H_2O$ (4.56 g) and $Fe(NO_3)_3 \cdot 9H_2O$ (7.21 g) were dissolved in 3.8 g oxalic acid and 40 $cm^3$ ethanol mixture at 80 °C. After stirring for 10 minutes, $Al(OC_2O_5)_3$ (9.2 $cm^3$) was added to a homogeneous transparent solution. Then the sol was slowly hydrolyzed by adding $H_2O/C_2H_5OH$ (60/40 V/V) mixture to the transparent solution and stirred at 110 °C for 16 hours to give transparent monolithic gel. The gel was dried at 120 °C in vacuum, powdered and calcined at 650 °C for 6 hours in air. The BET surface area of the fresh catalyst was 147.8 $m^2\ g^{-1}$.The actual phases identified for fresh catalyst were characterized by XRD and the different identified phases were $Fe_2O_3$ monoclinic, $MnO_2$ hexagonal, $MnAl_2O_4$ cubic and $Al_2O_3$ monoclinic. The sample after the FT reaction was also characterized and different identified phases were FeC orthorhombic, $MnAl_2O_4$ cubic, $Fe_2O_3$monoclinic, $Al_2O_3$ monoclinic and C hexagonal.

Also the catalysts were prepared by incipient wetness impregnation of $Al_2O_3$ with aqueous iron nitrate and manganese nitrate solutions. The $Al_2O_3$ support was first calcined at 600 °C in flowing air for 6 hours before impregnation. For 50%Fe/50%Mn/$Al_2O_3$ catalyst, the solution of proper amount of iron nitrate (5.53 g) and manganese nitrate (3.49 g) was prepared and directly dispersed through a spray needle onto the support. The impregnated support was then dried at 120 °C for 16 hours. In order to obtain the final catalyst, the precursor was then calcined at 550 °C for 6 hours. The BET surface area of the fresh catalyst was 127.9 $m^2\ g^{-1}$. The actual phases identified for fresh catalyst were $Fe_2O_3$ monoclinic, $MnO_2$, $Mn_2O_3$cubic, $AlFeO_3$orthorhombic and $Al_2O_3$ tetragonal. The sample after the FT reaction was also characterized and the different identified phases were $Fe_3C$ orthorhombic, $Fe_2C$ monoclinic, $Mn_2O_3$ orthorhombic, $FeFe_2O_4$ monoclinic, $MnAl_2O_4$/MnO, $Al_2O_3$ cubic.

Fig. 1 illustrates the XRD pattern for the fresh and used catalysts. The catalyst phase that exists is strongly dependent on the activation procedure employed. Activation with hydrogen, carbon monoxide or synthesis gas generally resulted in the rapid formation of metallic oxides especially $Fe_2O_3$ as an active phase.[22] With additional time, the $Fe_2O_3$ is converted to metallic iron in the case of hydrogen pretreatment or various iron carbides with carbon monoxide or synthesis gas pretreatment.[22–25] It is accepted that the oxidic and carbide phases are active in FTS for conversion of synthesis gas to olefins. It

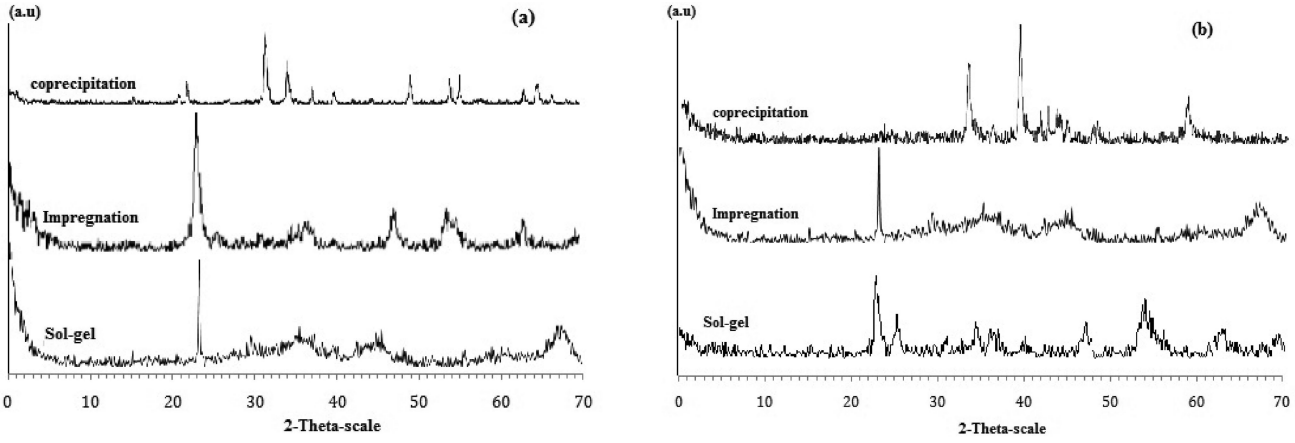


Fig. 1 – *XRD patterns of Fe/Mn/$Al_2O_3$ catalysts a) before and b) after the FTS test*

has also been reported that the formation of iron carbides results in high FTS activity, and the magnetite ($Fe_3O_4$) is the most active phase for water gas shift reaction.[26–30] Oxide phases are highly selective for the production of olefins, and carbide phases are active in the hydrogenation of CO.[31,32]

### Apparatus and data analysis

The catalyst tests were carried out in a micro-fixed-bed reactor (i.d. 7 mm and catalyst height bed ($H_b$) is 40 mm) under operating conditions as follows: pressure 6 bar, inlet $H_2$/CO ratios 1, temperature 220–260 ºC, and gas hourly space velocity 4500 $cm^3(STP)h^{-1}g_{cat}^{-1}$. More details about the reactor set up, as well as a schematic diagram, have been discussed in literature.[33–36] To summarize, the fresh catalyst was crushed and sieved to 0.25–0.36 mm (40–60 ASTM mesh) in size. The weight of the catalyst loaded was 1 g. To achieve a more uniform bed temperature, the catalyst was diluted using quartz sand with the same mesh size range. The volume ratio of catalyst to quartz sand was 1:4. Reduction of the catalyst was done in a $H_2$–$N_2$ flow (1800 $cm^3(STP)\ h^{-1}g_{cat}^{-1}$ for each) at atmospheric pressure and at 350 °C for 16 hours with a heating rate of 3 °C $min^{-1}$ at ambient temperature. The catalyst was then cooled to 180 °C and flushed with $N_2$ before the temperature was increased to desirable temperature. The GHSV of all the experiments were carried out at 4500 $cm^3(STP)\ h^{-1}g_{cat}^{-1}$, which is safe to eliminate the external mass transfer limitations.[35] Then the feed gas was introduced. Reactant and stream products were analyzed on line using a Varian gas chromatograph (Star 3600CX). The CO conversion (%) was calculated based on the fraction of CO that formed carbon containing products according to:

$$\text{CO conversion } (X_{CO}\%) = \frac{\sum n_i M_i}{M_{CO}} \times 100$$

Where $n_i$ is the number of carbon atoms in product i, $M_i$ is the percentage of product i and $M_{CO}$ is the percentage of carbon CO in feed stream. The selectivity (S) of product i, is based on the total number of carbon atoms in the product and is therefore defined as:

$$\text{Selectivity } (S_i\%) = \frac{\sum n_i M_i}{n_i M_i} \times 100$$

In this research, the carbon number distributions of Fischer–Tropsch products on iron/manganese catalysts were studied by using an Anderson–Schulz–Flory (ASF) distribution with one chain growth probabilities:

$$\frac{W_n}{n} = (1-\alpha)^2 \alpha^{n-1}$$

Where $W_n$ is the weight fraction of the products with n carbon number and $\alpha$ is the chain growth probability or growth factor. The logarithmic form of this kinetic expression is shown below:

$$\log\left(\frac{W_n}{n}\right) = \log(2\ln\alpha) + n\log(\alpha)$$

According to the equation, a plot of log ($W_n$/n) versus n gives a straight line (ASF plot) and the chain growth probability $\alpha$ can be calculated from the slope of the ASF distribution. Typically, the entire range from $C_2$ to $C_{15}$ was used to calculate $\alpha$.

## Results and discussion

### Catalyst characterization

Characterization of the 1Fe/1Mn/$Al_2O_3$ catalysts precursor was also carried out to measure the losses of weight as the temperature of the sample was increased. The TGA/DSC curves for these catalysts precursor are shown in Fig. 2.

For co-precipitated catalyst precursors, the thermogravimetric curves seemed to indicate three-stage decomposition. The first stage was considered to be due to the removal of adsorbed water (40–110 °C) and the second stage was due to the decomposition of hydroxyl bimetallic or nitrate precursor (250–375 °C), respectively. The peak around 525–575 °C was due to the decomposition of $MnCO_3$ or $Fe_2CO_3(OH)_2$ to oxides of iron and manganese phases ($Mn_5O_8$, $Fe_2O_3$ and $Mn_2O_3$) which were identified by XRD technique. The TGA curves were involved with total overall weight loss of ca. 55.2 wt.%. the exothermic peak at lower temperatures (40−120 °C) represented the removal of the physically adsorbed species and dehydration from the catalyst precursor. The second endothermic peak at around 175−275 °C was due to the decomposition of nitrate compounds. The peak around 375 °C was due to the full decomposition of nitrate compounds to oxides.

The TGA and DSC curves of the dried gel precursor show a total weight loss of 29.6% during continuous heating from room temperature up to 600 °C. In this range, for a typical gel-derived sample, the evaporation of the solvents and the subsequent pyrolyis and/or burning or residual organic molecules generally occurred.[37] For the catalyst precursor, two major weight losses were observed. The first weight loss, from 100 °C to 190 °C could be related to the evaporation, from open pores of water and alcohol physically trapped in the gels. The sec-

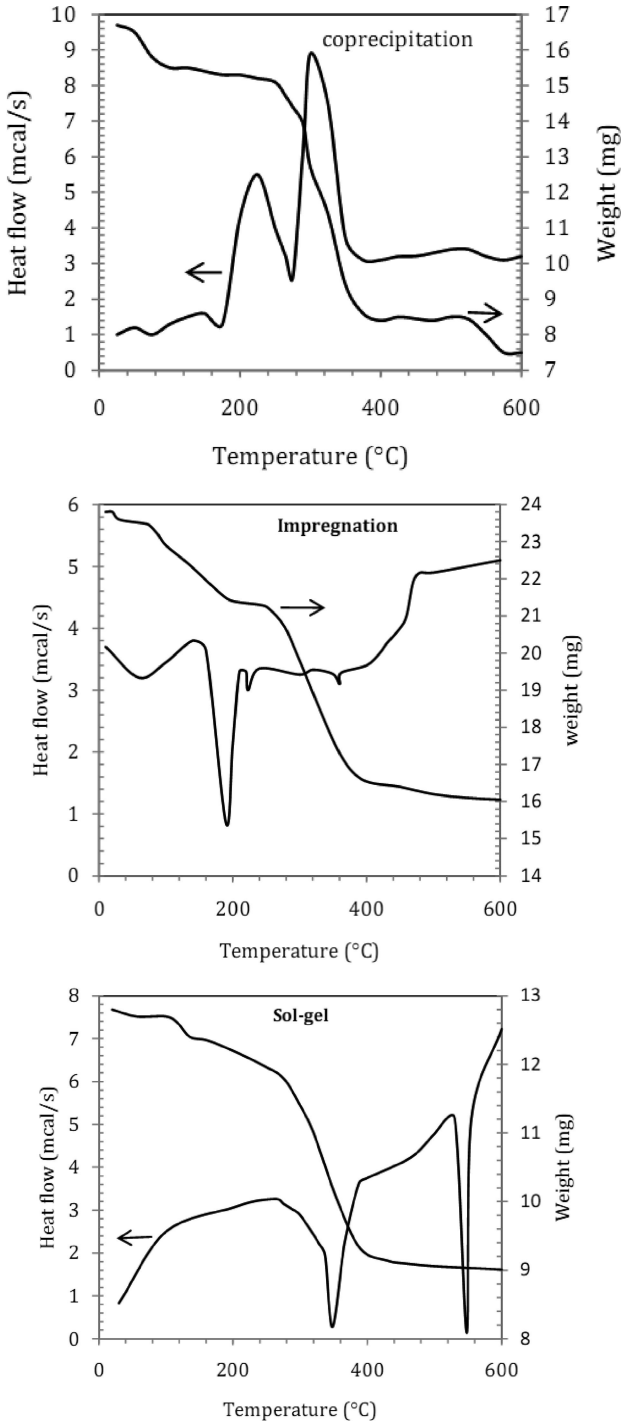


Fig. 2 – *TGA and DSC curves for various iron–manganese catalyst precursors*

ond weight loss at a range of 245 °C to 400 °C was likely to be caused by two overlapped processes: the burning of residual organic groups such as dehydroxylation reaction of structural OH contained in the metal oxyhydroxides, in the gels and the decomposition of the metal nitrates. This is in agreement with what has been reported.[38] The DSC measurement provided further evidence for the presence of the various species and evaluates their thermal behavior. As shown in Fig. 2, the exothermic peak at lower temperature (350 °C) represented the evaporation of the physically adsorbed water and alcohol from the gels, while the peak at the higher temperature (550 °C) solely represented the decomposition of the nitrates and hydroxylate. These two exothermic transitions, which were accompanied by weight loss, were interpreted on the basis of thermogravimetric analysis results.

For impregnated catalyst precursor, the weight losses obtained from TGA measurements were found to agree fairly well with those expected for the decomposition of nitrate compounds to oxides. For this catalyst precursor, the thermogravimetric curve seemed to indicate three-stage decomposition. The first stage was considered to be caused by the removal of adsorbed species and dehydration (30–60 °C). The second stage (70−190 °C) was due to the first decomposition of nitrate compounds. More $Ni(NO_3)_2$ and $Fe(NO_3)_3 \cdot 9H_2O$ decomposed at higher temperature. The peak around 260−400 °C was due to the full decomposition of nitrate compounds to oxides of iron and nickel phases ($MnO_2$, $Mn_2O_3$ and $Fe_2O_3$) which were identified by XRD technique. The TGA curve was involved with a total overall weight loss of ca. 32.5 wt%. As depicted the exothermic peak at lower temperatures (160−210 °C) represented the removal of the physically adsorbed species and dehydration from the catalyst precursor. The second peak at around 210−240 °C was due to the decomposition of nitrate compounds. The endothermic peak at 360 °C was due to the full decomposition of nitrate compounds to oxides.

## FTS performances

### Catalyst activity and stability

The activities of Fe/Mn catalysts prepared by different technique with time on stream (T.o.S) at three temperature levels (220, 240, 260 ºC) are shown in Fig. 3. The activity of catalyst for CO conversion was significantly promoted by change in

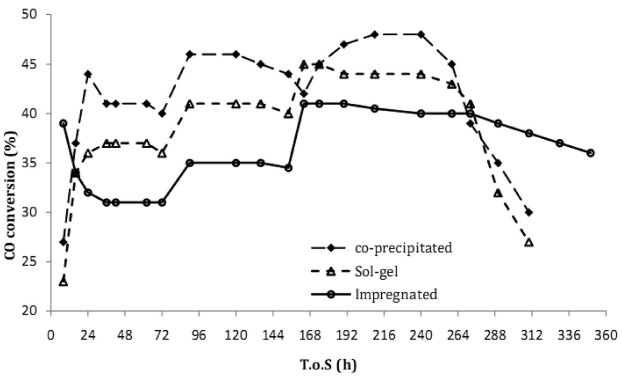


Fig. 3 – *Variation of activity and stability as a function of time on stream over Fe-Mn/$Al_2O_3$ at T = 220, 240, 260 ºC, p = 6 bar, GHSV = 4500 $h^{-1}$, $H_2/CO = 1$ (temperature increasing at 90 and 164 hr)*

preparation method from impregnation to co-precipitation. As shown, the CO conversion increased and reached to a stable level only after about 24 hours for all catalysts. For co-precipitated Fe/Mn, the CO conversion begins at 41% at 220 ºC then increases to 46% at 240 ºC after 90 hours. In this period, activity declined about 8%. After 164 hours, temperature increased to 260 ºC, and conversion enhanced to 45% and rapidly decreased to about 39% at 264 hours on stream. It seems that this catalyst is more sensitive to temperature. In the case of the sol-gel Fe/Mn catalyst, the CO conversion initially stabilized at 36% at 220 ºC in 48 hours and gradually increased to about 41% after a period of 144 hours at 240 ºC. After increasing to 260 ºC, conversion promoted to 45% and maintained stable thereafter to 264 hours, and suddenly depleted to 37%. For the impregnated Fe/Mn catalyst, the initial CO conversion begins at 32%. It further increased to about 35% after the second temperature increasing and maintained stable thereafter. In the third temperature increasing, conversion was 41% and stable after 290 hours. Generally, the increase in the reaction temperature led to the increase in the catalytic performance. Furthermore, it was shown that the reaction temperature should not be too low. At low reaction temperatures, the CO conversion was low, so it caused a low catalytic performance. On the other hand, increasing the reaction temperature leads to the formation of amounts of coke as an unwanted product.

It is evident that initial CO conversions of impregnated catalyst are lower but better in stability than in the case of the two other catalysts. It can be concluded that co-precipitated with the highest BET surface area has the highest conversion, and also impregnated catalyst shows the lowest C phases in used catalyst causing more stability in FTS. It is well-known that the higher FTS activity of the Fe-Mn catalyst in a fixed-bed reactor would result in much higher $H_2$/CO in the outlet than that in the inlet due to the integral effect.[39] Dwyer and Haredenergh[40] suggested that the competitive conversion of the reactive surface carbon to the surface polymeric carbon or graphitic carbon over the iron carbide surface determines the catalyst lifetime. Also, it is noticed that the C-C coupling of the surface carbon is more favorable thermodynamically while the surface hydrogen will hinder C-C coupling and prevent the deactivation of iron carbide surface.

For a better understanding of the deactivation behavior, the change in the methane and $C_{5+}$ selectivities has been plotted as a function of reaction time in Fig. 4 for all catalysts. As shown in this figure, for co-precipitated and impregnated catalysts, methane selectivity gradually declined about 4.5% and 4.7 respectively, while for sol-gel catalyst

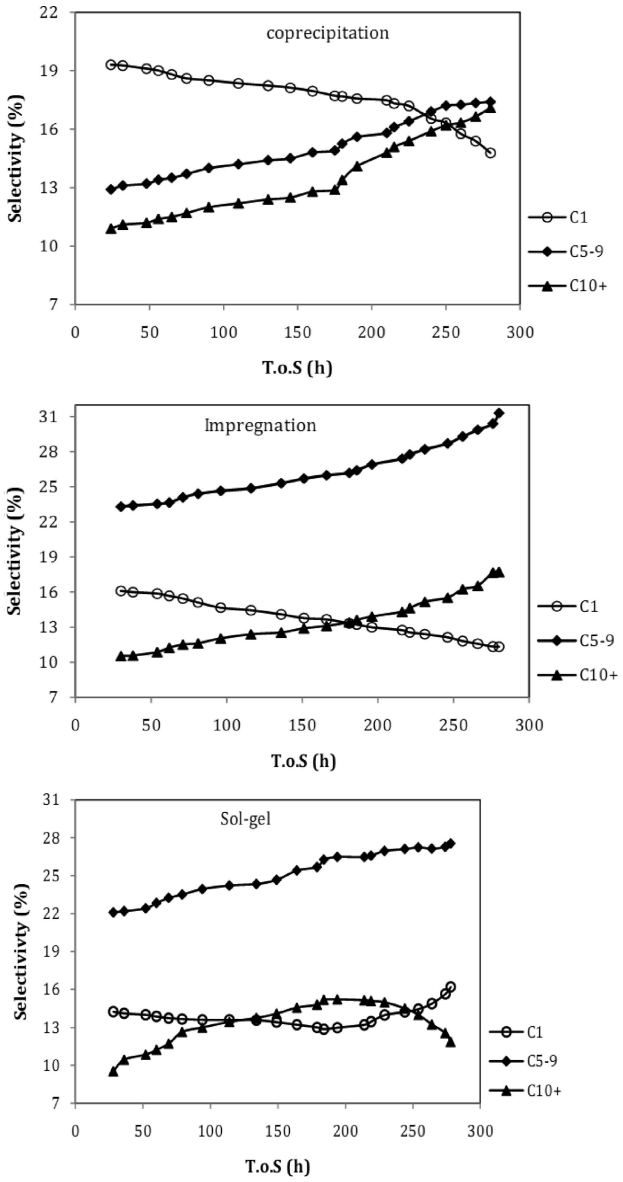


Fig. 4 – *Evolution with time on stream of the activity and selectivity measured over the various Fe/Mn/$Al_2O_3$ catalysts (T = 220 °C, p = 6 bar, $H_2$/CO molar feed ratio = 1, GHSV = 4500 cm³ (STP) $h^{-1}g_{cat}^{-1}$)*

methane selectivity remained constant with increasing in time up to 200 h. In contrast, $C_{5-9}$ selectivity (co-precipitated: 12.9 → 17.4, sol-gel: 22.1 → 27.5 and impregnated: 23.3 → 31.7) and $C_{10+}$ slightly increases by about 4.3% and 5.4% and 7.2, respectively during this time.

It has been shown that longer time enhanced agglomerate size growth during reaction conditions[41,42] which may be due to the possible existence of the bulk iron carbides FeC, as it could be detected by XRD patterns hence the larger particles were more selective to higher molecular weight hydrocarbons and smaller iron particles were selective to methane and light gaseous hydrocarbons[43–46] and the water-gas shift (WGS) reaction was faster on

smaller pellets.[47] However, M.A. McDonald[48] had reported in reverse results that large Fe particles produced a lower fraction of high hydrocarbon in the product and showed a greater tendency for deactivation and loss of $C_{2+}$ selectivity than small particles.

It is well-known that H and CO coverage play essential roles in the reactivity and selectivity of FT synthesis. CO and $H_2$ reactants should be supplied swiftly for hydrocarbon chain growth in the Fischer–Tropsch synthesis before the initial product, methane detached from the catalyst surface. Methane may face the reactants which will take part in the propagation reaction with $CH_4$ to produce long-chained hydrocarbons while attached to the surface. However, if $C_1$ desorbs from the catalyst before facing reactants, the reactants will react with each other to produce more $C_1$. Thus, a sufficient supply of reactants to the catalyst surface is very significant for hydrocarbon chain growth.[49] The XRD results showed that for sol-gel catalyst the amount of coke was higher than in the case of the two other catalysts. This could be related to $CH_4$ production (highly exothermic) followed by the coke formation on the catalyst surface, which resulted in the sharp increase of the reaction temperature and the catalyst deactivation.[50] It implied that the sol-gel catalyst loses the tendency of reactants; CO and $H_2$; chemisorptions at the end period of T.o.S. Therefore, deactivation rate of the smaller iron particles, which are selective for methane production, is higher than that of the larger particles. Therefore, these particles deactivated first, leading to increase in $C_{5+}$ selectivity and suppression of methane production. Also, The BET specific surface area of the co-precipitated, sol-gel and impregnated catalysts after T.o.S were found to be 152.3 → 150.7 $m^2 g^{-1}$, 147.8 → 136.5 $m^2 g^{-1}$ and 127.9 → 125.1 $m^2 g^{-1}$ respectively, which were in comparison with the BET results of the fresh catalysts and no significant change in the specific surface area was observed for co-precipitated and impregnated catalyst, but for the sol-gel catalyst sintering could be another deactivation reason.

### *Hydrocarbon selectivity*

The effects of preparation technique on the hydrocarbon product distribution of three catalysts are depicted in Fig. 5. It illustrates that the catalyst incorporated with co-precipitated method, had high selectivity to methane, $CO_2$ and $C_2$–$C_4$, whereas the selectivity to $C_5$–$C_9$was the lowest. The sol-gel catalyst suppressed the selectivities to methane but enhanced the selectivity to $C_5$–$C_9$ as compared with co-precipitated catalyst. Considering the impregnated catalyst, this catalyst suppressed WGS reaction and also the selectivity to $C_2$–$C_4$ but promoted the

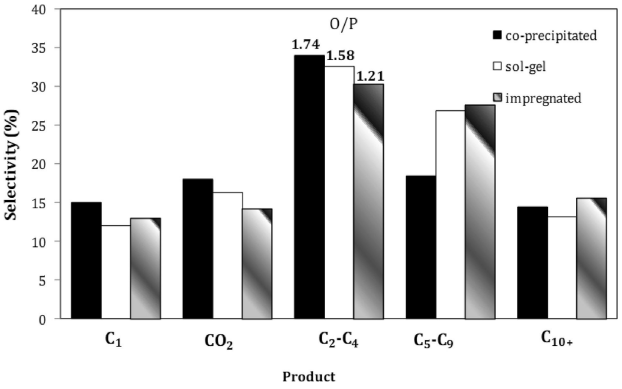


Fig. 5 – *Comparison of catalysts performance, Reaction condition: T = 220 ºC, p = 6 bar, GHSV = 4500 cm³ (STP) $h^{-1}$ $g_{cat}^{-1}$, $H_2/CO = 1$*

selectivity to high hydrocarbon compared with the two other catalysts.

It is widely accepted that iron carbides are the active phases,[51–54] which provide the active sites for CO activation and hydrogenation and oxide phases are highly selective for the production of olefins. Thus the content of $Fe_xC$ is important to form the active site at which the carbon atoms are hydrogenated and hence influence the formation of Fischer–Tropsch synthesis. At the same time, there is evidence[54,55] that the bulk carbide does not appreciably participate in the hydrocarbon synthesis. As for inactive carbons, some are inert while some are notorious poisons, such as graphite or coke. Zhang et al[56] found that there is a good correlation between the chemisorptions of $H_2$ or CO and the corresponding feed gas conversion activity in FTS reaction. Meanwhile, the methane selectivity is correlated with the hydrogenation capability of catalysts, indicating that the surface H concentration has an important effect on the selectivity of hydrocarbons.

## Chain growth

The quantitative description of FTS product distribution mathematically as a polymerization reaction, generally believed to form stepwise by insertion or addition of $C_1$ intermediates with constant growth probability, is given by the Anderson–Schulz–Flory (ASF) distribution.[57,58] The carbon number distribution of the products formed on iron-manganese catalysts are represented in Fig. 6. The product distributions were discussed by using the plot of Wn/n~n and the chain growth probability $\alpha$ can be calculated from the slope of the ASF distribution. The results demonstrate the changes observed in the product distributions when the catalyst is prepared by a different technique. It could be deduced that impregnated Fe-Mn has the greatest $\alpha = 0.786$, however for co-precipitated and sol-gel catalyst chain growth probability is equal to 0.760

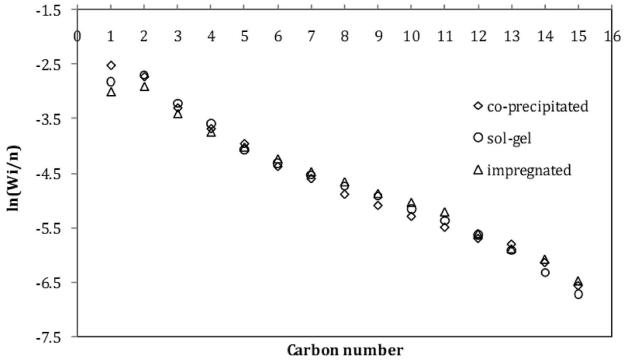


Fig. 6 – *Distribution of hydrocarbon with different carbon number for three types of the catalysts in the fixed-bed reactor*

and 0.761 respectively where $R^2$ as the amount of variance was more than 0.98 for all catalyst and F-test as the ratio of the mean regression squares and the mean residual squares was $F_{0.5}(4,28) = 2.71$<F-test(impregnated) = 145.2<F-test(co-precipitated) = 148.3<F-test(sol-gel) = 149.6. The results could also lead to the conclusion that the co-precipitated and sol-gel catalysts were preferential for chain termination to produce light hydrocarbons while the impregnated was preferential for the chain growth and the production of heavy hydrocarbons. It is well-known that the weakened surface basicity of iron-based catalyst can suppress the dissociative adsorption of CO, promote the adsorption of $H_2$, and retard the chain propagation reaction.[59] Also, higher chain growth probability seems to indicate $\alpha$-olefin readsorption on the growth sites, as favored by low secondary olefin hydrogenation and isomerization, high wax yield and long residence time.[39, 60]

## Conclusions

Three Fe-Mn/$Al_2O_3$ catalysts were prepared by three different preparation techniques, i.e. co-precipitates; sol-gel and impregnation to investigate activity and selectivity behavior during Fischer–Tropsch Synthesis (FTS) in a fixed-bed reactor and the following results were obtained:

1. As compared with co-precipitates and sol-gel Fe-Mn catalysts, the CO conversions of impregnated catalyst were the lowest but much more stable than the other two catalysts.

2. Co-precipitated and sol-gel catalysts enhanced light olefins as compared with impregnated.

3. Sol-gel Fe-Mn suppressed the methane formation better than the two other catalysts.

4. Impregnated catalyst suppressed WGS activity and enhanced the high hydrocarbon selectivities and had the highest chain growth probability.

## References:


1. *Rahimpour, M. R., Jokarand, S. M., Jamshidnejad, Z.,* Chem. Eng. Res. Des. **90** (2012) 383–396.
2. *Rafiee, A., Hillestad, M.,* Comput. Chem. Eng. **39** (2012) 75– 83.
3. *Glasser, D., Hildebrandt, D., Liu, X., Lu, X., Masuku, C. M.,* Curr. Opin. Chem. Eng. **1** (2012) 296–302.
4. *Bae, J.W., Park, S. J., Kang, S. H., Lee, Y. J., Jun, K. W., Rhee, Y. W.,* J. Ind. Eng. Chem. **15** (2009) 798–802.
5. *Nakhaei Pour, A., Housaindokht, M. R., Tayyariand, S. F., Zarkesh, J.,* J. Nat. Gas. Chem. **19** (2010) 284–292.
6. *Maureen, E., Jack, C. F.,* Appl. Catal., A **57** (1990)L5–L8.
7. *Malesaa, R., Baerns, M.,* Ind. Eng. Chem. Res. **27** (1978) 279–283.
8. *Mirzaei, A. A., Faizi, M., Habibpour, R.,* Appl. Catal., A **306** (2006) 98–107.
9. *Mirzaei, A. A., Beigbabaei, A., Galavy, M., Youssefi, A.,* Fuel Process. Technol. **91** (2010) 335–347.
10. *Mirzaei, A. A., Shahriari, S., Arsalanfar, M.* , J. Nat. Gas. Sci. Eng. **3** (2011) 537–546.
11. *Bai, L., Xiang, H. W., Li, Y. W., Han, Y. Z., Zhong, B.,* Fuel **81** (2002)1577–1581.
12. *Wang, C., Wang, Q. X., Sun X. D., Xu, L. Y.,* Catal. Lett. **105** (2005) 93–101.
13. *Wenping, M., Edwin, L. K., James, W., Dadyburjor, D. B.,* Energy Fuels **20** (2006) 2299–2307.
14. *Bromfield, T. C., Visagie, R.,* U.S. Patent WO2005/049765A1, (2005)
15. *Lohitharn, N., Goodwin,J. G.,* J. Catal. **260** (2008) 7–16.
16. *Lohitharn, N., Goodwin, J. G., Lotero, E.,* J. Catal. **255** (2008) 104–113.
17. *Jensen, K. B., Massoth, F. E.,* J. Catal. **92** (1985)109–118.
18. *Li, T. Z., Yang, Y., Zhang, C. H., An, X., Wan, H. J., Tao, Z. C., Xiang, H. W., Li, Y. W., Yiand, F., Xu, B. F.,* Fuel **86** (2007) 921–928.
19. *Van Dilk, W. L., Niemantsverdriet, J. W., Van der Kraan, A. M., Van der Baan, H. S.,* Appl.Catal. **2** (1982) 273–288.
20. *Leithand, I. R., GHowden, M.,* Appl. Catal. **37** (1988) 75–92.
21. *Mirzaei, A. A., Vahid, S., Feyzi, M.,* Adv. Phys. Chem. **2009** (2009) Article ID 151489, doi:10.1155/2009/151489
22. *O'Brien, R. J., Xu, L., Milburn, D. R., Li, Y. X., Klabunde, K. J., Davis, B.H.,* Top. Catal. **2** (1995) 1–15.
23. *Dry, M. E., Boudart, J. R.,* Catal. Sci. Tech. New York: Springer-Verlag Press, 1981.
24. *Anderson, R. B.,* The Fischer-Tropsch synthesis. Orlando: Academic Press, 1984.
25. *Bukur, D. B., Koranne, M., Lang, X., Rao, K. R. P. M., Huffman, G. P.,* Appl. Catal., A **126** (1995) 85–113.
26. *Botes, F. G.,* Appl. Catal., A **328** (2007) 237–242.
27. *Van der Laan, G. P., Beenackers, A. A. C. M.,* Appl. Catal., A **193** (2000) 39–53.
28. *Wang, Y.N., Ma, W. P., Lu, Y. J., Yang, J., Xu,Y. Y., Xiang, H. W., Li, Y. W., Zhao, Y. L., Zhang, B. J.,* Fuel **82** (2003) 195–213.
29. *Teng, B. T., Chang, J., Yang, J.,Wang, G., Zhang, C. H., Xu, Y.Y., Xiang, H. W.,Li, Y. W.,* Fuel **87** (2005) 791–800.
30. *Guo, X. H., Liu, Y., Chang, J., Bai, L., Xu, Y. Y., Xiang, H .W., Li, Y. W.,* J. Nat. Gas. Chem. **15** (2006) 105–114.
31. *Shroff, M. D., Kalakkad, D. S., Coulter, K. E., Kohler, S. D., Harrington, M. S., Jackson, N. B., Sault, A. G., Datye, A. K.,* J. Catal. **156** (1995) 185–207.

32. *Zhang, H. B., Schrader, G. L.,* J. Catal. **95**(1985) 325–332.
33. *Atashi, H., Fazlollahi, F., Sarkari, M., Mirzaei, A. A., Allahyari, S.M.,* Inter. J. Chem. React. Eng. **9** (2011) article A88.
34. *Feyzi, M., Irandoust, M., Mirzaei, A. A.,* Fuel Process. Technol. **92** (2011) 1136–1143.
35. *Arsalanfar, M., Mirzaei, A.A., Atashi, H., Bozorgzadeh, H. R., Vahid, S., Zare, A.,* Fuel Process. Technol. **96** (2012) 150–159.
36. *Shiva, M., Atashi, H., Farshchi Tabrizi, F., Mirzaei, A. A.,* J. Ind. Eng. Chem. **18** (3) (2012) 1112–1121.
37. *Brinker, C., Schere, S. W.,* Sol–Gel Science: The Physics and Chemistry of Sol–Gel Processing, Academic Press, New York, 1990.
38. *Cornell, R. M., Schwertmann, U.,* The Iron Oxide: Structure, Properties, Reactions, Occurrence and Uses, VCH Publishers, Weinheim and New York, 1996.
39. *Liu, Y., Bo-Tao, T., Xiao, H., Ying, Li., Jie, C., Lei, T., Xu, H., Yu, W., Hong, X., Yuan-Yuan, X., Yong-Wang, L.,* J. Mol. Catal. A: Chem. **272** (2007) 182–190.
40. *Dwyer, D. J., Hardenbergh, J. H.,* J. Catal. **87**(1984) 66–76.
41. *Feyzi, M., Irandoust, M., Mirzaei, A. A.,* Fuel Process. Technol. **92** (2011) 1136–1143.
42. *Feyzi, M., Jafari, F.,* J. Fuel. Chem. Technol. **40**(2012) 550–557.
43. *Sarkari M., Fazlollahi F., Atashi H, Mirzaei A. A., Hosseinpour V.,* Fuel Process. Technol. **97** (2012) 130–139.
44. *Feyzi, M., Mirzaei, A. A., Bozorgzadeh, H. R.,* J. Nat. Gas. Chem. **19** (2010) 341–353.
45. *Sarkari, M., Fazlollahi, F., Razmjooie, A., Mirzaei, A. A.,* Chem. Biochem. Eng. Q. **25** (2011) 289–297.
46. *Mirzaei, A. A., BeigBabaei, A., Galavy, M., Youssefi, A.,* Fuel Process. Technol. **91** (2010) 335–347.
47. *Liu, Z. T., Li, Y. W., Zhou, J. L, Zhang, Z. X., Zhang, B. J.,* Appl. Catal., A **161** (1997) 137–151.
48. *McDonald, M. A., Storm, D. A., Boudart, M.,* J. Catal. **102** (1986) 386–400.
49. *Fogler, H. S.,* Elements of Chemical Reaction Engineering, 2nd ed. Prentice-Hall Int., London, 1992.
50. *Adesina, A. A.,* Appl. Catal., A **138** (2) (1996) 345–367.
51. *Cao, D. B., Li, Y. W., Wang, J. G., Jiao, H. J.,* J. Phys. Chem. C **112** (2008) 14883–14890.
52. *Rao, K. R .P., Huggins, F. E., Mahajan, V., Huffman, G. P., Rao, V. U., Bhatt, B. L., Bukur, D. B., O'Brien, R. J.,* Top. Catal. **2** (1995) 71–78.
53. *Mansker, L. D., Jin, Y., Burker D. B., Datye, A. K.,* Appl. Catal., A **186** (1999) 277–296.
54. *Li, S., Meitzner, G. D., Iglesia, E.,* J. Phys. Chem. B **105** (2001) 5743–5750.
55. *Kummer, J. T., DeWitt, T. W., Emmett, P. H.,* J. Am. Chem. Soc. **70** (1948) 3632–3643.
56. *Stockwell, D. M., Bianchiand, D., Bennett, C. O.,* J. Catal.**113** (1988) 13–24.
57. *Chenghua, Z., Guoyan Z., Kangkai, L., Yong, Y., Hongwei, X., Yongwang, Li,* J. Mol. Catal. A: Chem. **328** (2010) 35–43.
58. *Anderson, R. B.,* In: P.H. Emmett (Ed.), Catalysis, vol. IV, Van Nostrandreinhold, New York, pp. 29–255, 1956.
59. *Henrici-Olivéand, G., Olivé, S.*, Angew. Chem. Int. Ed. **15** (1976) 136–141.
60. *Miller, D., GandMoskovits, M.,* J. Phys. Chem. **92** (1988) 6081–6085.